ACS APPLIED MATERIALS & INTERFACES

Research Article

www.acsami.org

Air Heating Approach for Multilayer Etching and Roll-to-Roll Transfer of Silicon Nanowire Arrays as SERS Substrates for High Sensitivity Molecule Detection

Yan Wang, Xiujuan Zhang,* Peng Gao, Zhibin Shao, Xiwei Zhang, Yuanyan Han, and Jiansheng Jie*

Institute of Functional Nano & Soft Materials (FUNSOM) & Collaborative Innovation Center of Suzhou Nano Science and Technology, Jiangsu Key Laboratory for Carbon-Based Functional Materials & Devices, Soochow University, Suzhou, Jiangsu 215123, P. R. China

Supporting Information

ABSTRACT: SiNW array represents an attractive system for construction of high-performance energy, electronic, and sensor devices. To meet the demand for flexible devices as well as address the concern about the full use of the Si material, large-area transfer of the SiNW array from growth substrate is very desirable. Here, we report a simple air heating approach to achieve the multilayer etched SiNW array. This method allows the fabrication of up to a five-layer (while perfectly three-layer) cracked SiNW array on single-crystalline Si wafer via a templateless metal-assisted etching approach. Fractures could happen at the crack position when an appropriate pressure was applied on the SiNW array, facilitating the wafer-scale layer-by-layer transfer of the SiNW array onto a flexible substrate through a low-cost and time-efficient roll-to-roll (R2R) technique. Further releasing of the SiNW array to other receiving substrates was accomplished with the aid of a thermal release tape. After modification with sliver nanoparticles (AgNPs), the flexible SiNW array showed great potential as a high-sensitivity surface-enhanced Raman spectroscopy (SERS) substrate for detecting rhodamine 6G (R6G) molecule with concentration as low as 10^{-9} M.

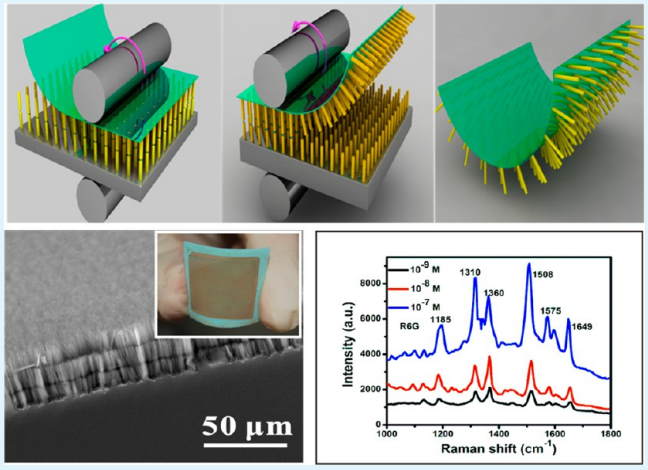

KEYWORDS: *multilayer etching, roll-to-roll transfer, silicon nanowire arrays, SERS substrates, rhodamine 6G (R6G)*

INTRODUCTION

One-dimensional (1D) semiconductor nanostructure arrays, nanostructures with uniform size and orientation, have attracted considerable interest because of the amazing properties arising from their distinct array structure.[1−3] The strong optical absorption, low laser emission threshold, short charge carrier collection length, and excellent electrical characteristics make the 1D semiconductor nanoarrays promising candidates for solar cell, photodetector, laser, and sensor applications.[4,5] Silicon is the most important semiconductor in current microelectronics and photovoltaics (PVs); therefore, silicon nanowire (SiNW) arrays have drawn a lot of attention in the past decade. Yang et al. demonstrated that a thin SiNW array with thickness less than 10 μm is capable of absorbing most of the incident light.[6] Lewis et al. also reported the high efficiencies of the SiNW array based solar cells owing to the unique radial p−n junction structure, which can greatly facilitate the carrier separation/transportation.[7] In light of this, various SiNW array based solar cells have been intensively studied recently, including SiNW p−n homojunction,[8] SiNW array/graphene Schottky junction,[9] and SiNW array/conductive polymer hybrid heterojunction solar cells ect.[10] The optimum efficiencies of over 10% have been achieved for these devices,[11] highlighting the great potential of the SiNW arrays as the building blocks for high-performance PV devices. On the other hand, SiNW arrays also show the promise in sensor applications.[12,13] When noble metals (silver or gold) were coated on the surface of H-terminated SiNWs, the SiNWs can serve as high-sensitive substrates for surface-enhanced Raman scattering (SERS) or fluorescence detection.[12] It has been reported that the SiNWs based SERS substrates could achieve an extremely strong Raman signal with a detection limit of about 600 rhodamine 6G (R6G) molecules.[13]

There are two major methods for the fabrication of SiNW arrays, i.e., top−down etching and the bottom−up epitaxial growth methods;[14−18] both of them can produce SiNW arrays with a high degree of vertical alignment. However, in comparison to the epitaxial method, the etching method

Received: October 6, 2013
Accepted: December 30, 2013
Published: December 30, 2013

shows the superiorities in terms of low cost and high throughput and has the potential for future large-scale applications. It is worth noting that in most cases the as-prepared SiNW arrays are tightly attached in series to the underlying growth/etching Si substrates,[19−21] and it remains a challenge to isolate the SiNW arrays for distinguishing their inherent properties. Considering the fact that the distinct properties of the array structure mainly arise from the SiNW array on the top[22,23] and that the thick Si substrate is not so useful except for the support of the SiNW arrays, it is expected that the consumption of Si material can be greatly reduced by separating the SiNW array from the underlying substrate, while maintaining its vertically aligned orientation, and then recycling the substrate for the fabrication of new SiNW array. To this end, one method used a razor blade to scratch the SiNW array from the substrate,[24] but this method is less efficient and only suitable for small-size applications. Peeling off SiNW array directly from the substrate was demonstrated;[25] however, polydimethylsiloxane (PDMS) had to be used to encapsulate the array first and the NW array must be long with large inter-wire spacing. Recently, Zheng et al. developed a hot water soaking method to achieve the vertical transfer of the SiNW array.[22] Nevertheless, the relatively long soaking time will inevitably increase the process complexity, and the SiNWs must have large diameter to withstand the long time hot water soaking process.

Herein, we report an alternative and yet simple, versatile, and high-yield approach to achieve the multilayer etching and roll-to-roll (R2R) transfer of SiNW arrays. Metal-assisted etching method was utilized to fabricate the SiNW array on single-crystalline Si wafer. By direct heating of the as-prepared SiNW array in air, Ag nanoparticles (AgNPs) could adhere on the side surfaces of the SiNWs; the lateral etching of the AgNPs in the following etching step resulted in the formation of a horizontal crack in the NWs. By repetition of the etching−air heating−etching process, multilayer etching of SiNW arrays with layer number up to 5 was realized. This method exhibited high flexibility and could be extended to the Si wafers with different conduction types, orientations, and doping levels. Notably, wafer-scale transfer of the multilayer SiNW array was demonstrated with a R2R approach. After surface modification with AgNPs, the SiNW array on flexible substrate showed promising applications as SERS substrate for high-sensitivity organic molecules detection. It is expected that the multilayer etched and transferred SiNW arrays will have important applications in future low-cost and flexible sensor devices.

EXPERIMENTAL DETAILS

Multilayer Etching of SiNW Arrays. The commercial 4 in. single-crystalline Si wafers were cut into 1 × 1 cm^2 pieces and ultrasonically cleaned in acetone, ethanol, and deionized (DI) water for 10 min, respectively. After being cleaned, the Si substrates were dipped into 5% HF aqueous solution for 2 min to form H-terminated surfaces. Then the substrates were immediately immersed into an Ag coating solution containing 4.8 M HF and 0.02 M $AgNO_3$ for 20−30 s to form a thin film of AgNPs on the substrates. After that, the substrates were rinsed with DI water to remove the extra Ag^+ and then etched in etchant composed of 4.8 M HF and 0.4 M H_2O_2. Once etched for a certain time, the substrates were taken out and rinsed with DI water several times and then dried in air by N_2 gas flow. A layer of SiNW array would be formed on the Si substrate after etching. The SiNW length depended on the etching time. In order to achieve multilayer etching of SiNW array, the as-prepared SiNW array was heated in air at 150 °C for about 30 min; part of the Ag film would be melted and some AgNPs were adhered to the side walls of SiNWs. Afterward, the Si substrate was put back into the etching solution for the second round etching and a horizontal crack would be formed where the AgNPs adhered after a given etching time. By repetition of the etching−air heating−etching steps, a multilayer SiNW array was formed on the Si substrate. Eventually, the residual Ag catalyst was removed by immersing the substrate into nitric acid (HNO_3/H_2O volume ratio of 1:1) for 15 min. In this work, to exploit the potential of this method, multilayer etching on Si wafers with different conduction types, orientations, and doping levels was investigated.

R2R Transfer of the Multilayer SiNW Arrays. A conventional laminating machine was employed for the R2R transfer of the SiNW arrays. In a typical process, the thermal released tape was pasted on the top of Si substrate with multilayer etched SiNW array on it. The tape, along with the SiNW array, was then passed through the laminating machine, and sufficient stress was applied on the substrate by the two rubber roller of the laminating machine. The tape was tightly adhered on the SiNW array after this process. Afterward, the thermal released tape was peeled off to vertically transfer the SiNW array from the underlying Si substrate.

Fabrication of AgNPs-Coated SiNW Arrays. To prepare the silver-plating solution, 1.5 mL of freshly prepared 5% NaOH solution was added to an aqueous solution of $AgNO_3$ (0.375 g in 45 mL of water) under vigorous stirring. Then the dark-brown precipitate was redissolved by slowly adding 1 mL of $NH_3{\cdot}H_2O$. Subsequently, the solution was cooled to 5 °C in an ice bath and an aqueous solution of D-glucose (0.540 g in 11 mL of water) was added to obtain the silver-plating solution.[26] The cleaned SiNW arrays with horizontal cracks were placed in H_2SO_4/H_2O_2 (volume ratio, 3:1) solution at room temperature for 30 min to obtain a hydroxyl surface. After a further cleaning with DI water, the SiNW arrays were immersed into a solution of 3-aminopropyltrimethoxysilane (ATPMS) (ATPMS/methanol volume ratio, 1:10) for 2 h. Afterward, the ATPMS modified SiNW arrays were dipped into a solution containing small gold nanoparticles (AuNPs, ∼10 nm) for 8 h. Then the SiNW arrays were decorated with AuNPs, which could control the silver deposition, ensuring a homogeneous growth of the AgNPs.[27] The AuNPs modified SiNW arrays were dried in the air. And then the top layer of the AuNPs decorated SiNW arrays was transferred to the flexible thermal released tapes by the aforementioned R2R transfer method. Finally, the transferred SiNW array on flexile tape was dipped into the silver-plating solution for about 3 min to deposit a thin AgNPs layer on the surface of SiNW array.

Material Characterization and SERS Measurements. The morphologies and structures of the SiNW arrays were investigated by scanning electron microscope (SEM, FEI Qnanta 200 FEG) and transmission electron microscope (TEM, FEI Tecnai G2 F20). The components were detected by energy dispersive X-ray spectrometry (EDS) attached on SEM. The reflection spectra of the SiNW array were recorded in the wavelength range of 300−1200 nm by using a UV−vis spectrophotometer (Lambda 750).

R6G dissolved in methanol with a concentration of 10^{-7}−10^{-9} M was selected as the probe molecule. An amount of 5 μL of methanol solution that contains various amounts of R6G molecules was dropped onto the flexible AgNPs-modified SiNW array. SERS spectra were detected on a Raman spectrometer (HORIBA Jobin Yvon LabRAM HR800). Raman spectra were collected by using the 633 nm radiation from an Ar ion laser as the excitation source. The laser beam was focused to a spot with a diameter of approximately 2 μm using a 50× telephoto lens. The data acquisition time was 8 s for one accumulation. The Raman scattering peak of Si wafer at 520 cm^{-1} was used to calibrate the spectrometer. Besides R6G, *p*-aminothiophenol (PATP) and crystal violet (CV) dissolved in methanol with different concentrations were also selected as the probe molecules. The detection processes were similar to that for R6G.

RESULTS AND DISCUSSION

Multilayer Etched SiNW Arrays with Horizontal Cracks. The SiNW arrays with well-controlled horizontal

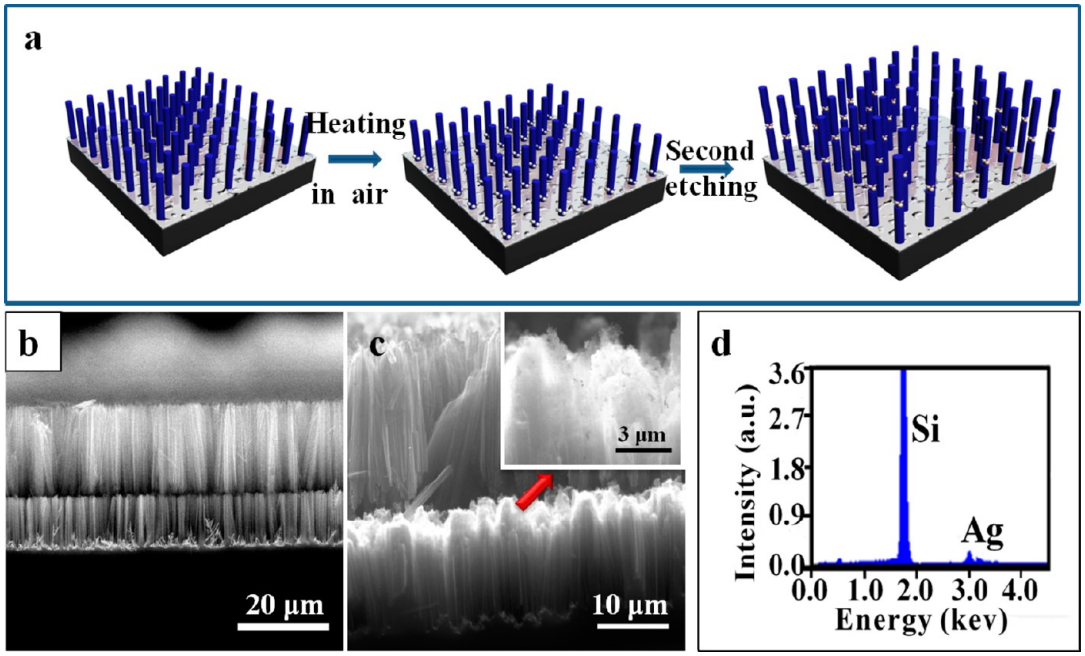

Figure 1. (a) Schematic illustration of the fabrication procedure for the multilayer SiNW array. (b) Cross-sectional view SEM image of the SiNW array with a horizontal crack. The n-type ⟨100⟩ Si wafer with resistivity of 1−2 Ω cm was used. (c) Enlarged SEM at the crack position. Inset shows that AgNPs with dark contrast existed at the crack position. (d) EDS analysis of the SiNW array at crack position.

cracks were fabricated via a very convenient way and can be realized on a large scale. The procedure for the fabrication of horizontally cracked SiNWs involves mainly three steps, as depicted in Figure 1a. First, the single-layer SiNW array was fabricated by Ag catalyzed chemical etching approach on single-crystalline Si wafer.[28] Second, the wafer was heated directly in air at 150 °C for about 30 min to break the Ag catalyst film and to allow some of the AgNPs to adhere to the side walls of SiNWs.[29] Finally, the horizontal crack was formed by returning the Si wafer back into the etching solution for second-round etching. Because of the enlarged contact area of adhered AgNPs to sidewalls of SiNWs, the adhered AgNPs preferred to etch along the lateral direction, resulting in the crack of the SiNWs. Figure 1b shows clearly a horizontal crack existing in the SiNW array. From the enlarged SEM, Figure 1c, the small AgNPs with dark contrast can be observed in the crack. In addition to the Si signal, EDS analysis on SiNW array at the crack position also reveals evident Ag peaks, verifying the existence of the AgNPS (Figure 1d).

In order to exploit the flexibility of the proposed air heating method, a wide range of Si wafers with different conduction types, crystal orientations, and doping levels were investigated, as shown in Figure 2. Previous studies have shown that the etching speed of Ag catalyst depends on the crystal orientations as well as the doping levels of the wafers;[28] etching speed of lightly doped Si wafer is a little faster than that of heavily doped Si wafer, while ⟨100⟩ Si wafer has higher etching speed than Si wafers with other orientations. Therefore, in this work, to ensure a similar array height for all the wafers, the etching time was optimized to be 30−40 min for lightly doped Si wafers while it was 40−50 min for heavily doped Si wafers. The etching time for ⟨110⟩ and ⟨111⟩ Si wafers was further prolonged to be 50−60 min. Therefore, the array height in each round etching is roughly in the range of 20−30 μm for all the wafers. From Figure 2, it is seen that cracked SiNW arrays can be formed on both n- and p-type Si wafers, and the doping levels have little influence on the formation of cracks. For the ⟨100⟩ Si wafers, the etched SiNW arrays are vertically aligned on the substrates and the cracks are parallel to the substrate planes. In contrast, the SiNW arrays etched from ⟨110⟩ and ⟨111⟩ Si wafers have a tilted orientation on the substrates. This phenomenon is observed in previous studies and can be attributed to the preferential etching along the ⟨100⟩ direction.[28] In spite of this, the crack lines can be clearly investigated in the SiNWs on ⟨110⟩ and ⟨111⟩ wafers and remain parallel to the substrate planes. However, close investigation on the cracks on ⟨111⟩ wafer indicates that the crack in each SiNW is still approximately vertical to the NW length direction (inset in Figure 2e, indicated by the dash lines), implying that the adhered AgNPs may still etch along one of the crystallographically equivalent directions of ⟨100⟩. More meaningfully, as shown in Figure 3, multiple cracks can be created along the SiNWs by repeating the air heating and solution etching steps. Parts a−d of Figure 3 show that in this way we can fabricate multilayer SiNW arrays with one to four horizontal cracks (two- to five-layer SiNW arrays). Nevertheless, we note that the top layer of the four- or five-layer cracked SiNW array tends to collapse because of the long solution etching time, in contrast to the perfect layered structure for three-layer cracked SiNW array. Therefore, the optimum layer number for the air heating method is about three layers. Meanwhile, the layer thickness in each layer can be readily tuned by adjusting the etching time in each step. From Figure 3c and Figure 3d, it is noted that the layer thickness decreases from 10 μm for first layer to 6 μm for second layer when the etching time is reduced from 20 to 15 min. Nevertheless, the layer thickness is restored to 10 μm when the etching time is prolonged to 20 min again for third-layer etching. The above results unambiguously demonstrate the versatility of the proposed air heating method.

It is worth mentioning that although a hot water soaking method has been developed previously to create cracks in the

dx.doi.org/10.1021/am4043883 | ACS Appl. Mater. Interfaces 2014, 6, 977−984

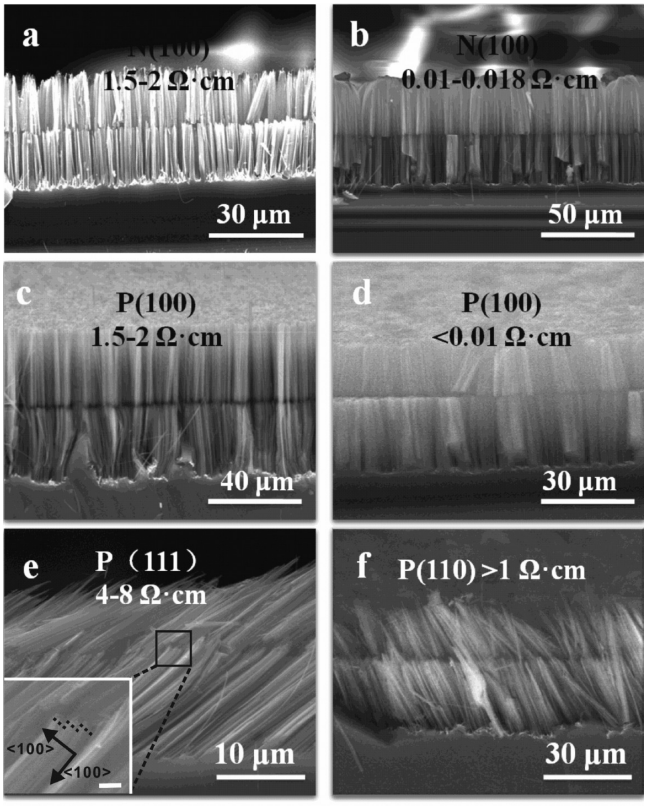

Figure 2. Cross-sectional view SEM images of the SiNW arrays with horizontal cracks prepared from (a) lightly doped n-Si ⟨100⟩ wafer with resistivity of 1.5−2 Ω·cm, (b) heavily doped n-Si ⟨100⟩ with resistivity of 0.01−0.018 Ω·cm, (c) lightly doped p-Si ⟨100⟩ wafer with resistivity of 1.5−2 Ω·cm, (d) heavily doped p-Si ⟨100⟩ wafer with resistivity of <0.01 Ω·cm, (e) lightly doped p-Si ⟨111⟩ wafer with resistivity of 4−8 Ω·cm, and (f) lightly doped p-Si ⟨110⟩ wafer with resistivity of >1 Ω·cm. Inset in (e) shows the enlarged SEM image of the cracked SiNWs. The dash lines indicate the crack directions in the NWs, which are approximately vertical to the length directions of NWs. Scale bar = 1 μm.

SiNW array,[22] SiNWs in this method were fabricated by using monolayer silica (SiO_2) spheres as template and have a relatively large diameter around 400 nm. The thick SiNWs have higher mechanical strength and therefore can retain the vertical alignment even after a long time hot water soaking process (75 °C, >3 h). This is particularly important for the multilayer etching of the SiNW array (layer number, ≥3). In present work, however, the SiNWs were fabricated via a templateless metal-assisted etching method; the thin NWs with diameter of 50−200 nm can hardly stand the hot water soaking. Figure S1 shows the SEM image of the cracked SiNW array fabricated by the hot water soaking method. It can be seen that the long time soaking (≥3 h) is necessary to generate a crack in SiNW array, while the top SiNW array has fully collapsed for three-layer SiNW array and the surfaces of the rest SiNWs become very rough because of the etching effect of hot water. In comparison to the hot water soaking method, the air heating approach is much simpler and more efficient. More importantly, the short air heating process (30 min) has little influence on the array structure of the SiNWs, making it possible to fabricate multilayer SiNW array with layer number up to 5 by this means (Figure 3d).

SiNW Arrays Transfer. Creation of a horizontal crack through SiNW arrays enables the controllable breakage of the

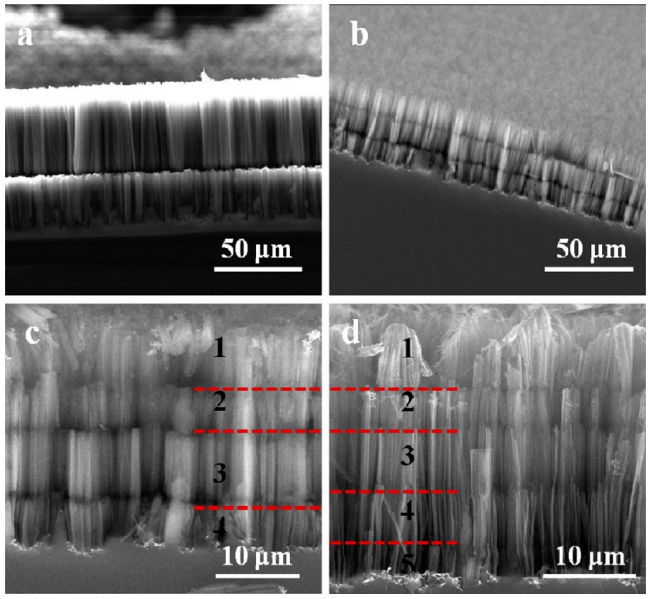

Figure 3. Cross-sectional view SEM images of the multilayer SiNW arrays with different layer number of (a) two layers, (b) three layers, (c) four layers, and (d) five layers. The numbers in (c) and (d) mark the different SiNW layers.

SiNWs at specified locations and also facilitates their transfer to other substrates. In this work, vertical transfer of the cracked SiNW arrays is achieved simply by attaching an adhesive tape at the top of the multilayer etched SiNW array and then peeling off the adhesive receiver substrate. Si is partially etched away at the crack location of the SiNWs, which weakens the connection between the top and bottom SiNW arrays. When the top SiNW array was attached to the tape and an appropriate pressure was applied, the SiNW array would fracture along the crack lines. The connection between the top SiNW array and the tape is stronger than its connection with the bottom SiNW array, allowing the full transfer of the top SiNW array to tape. Interestingly, the use of the adhesive tape as the receiver substrate offers the possibility of transferring the SiNW array with a cost- and time-effective R2R method. Thermal release tape was utilized here because of its good stickiness. In addition, the thermal release tape will become totally inadhesive as long as it is heated to above 120 °C. This means that the SiNW array can be readily transferred from the tape to any target substrates, facilitating the device applications of the SiNW array.

Figure 4a illustrates the procedure for the R2R transfer of the SiNW array. There are three essential steps in this approach: (i) adhesion of the tape to the top layer of the cracked SiNW array on Si substrate. The Si substrate and the tape are then passed through a R2R system; the tape will be tightly adhered to the SiNW array due to the pressure force applied by the two rubber rollers. The pressure force could be controlled by adjusting the interspace of the rollers. Normally, we set the interspace to a value that is a little bit smaller than the thickness of the Si substrate to obtain an appropriate pressure. The pressure cannot be too high; otherwise, the Si substrate will be crushed because it has become very fragile after multiround etching. After passing through the R2R system, the SiNWs will fracture at the crack positions and are ready for transfer at the next step. (ii) The next step is release of the top SiNW array from the Si substrate. After step i, the top SiNW array can be completely

dx.doi.org/10.1021/am4043883 | ACS Appl. Mater. Interfaces 2014, 6, 977−984

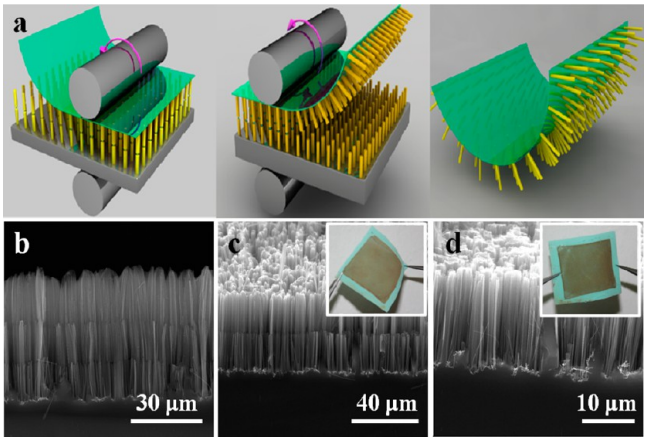

Figure 4. (a) Schematic illustration shows the roll-to-roll transfer process of the multilayer SiNW array. Cross-sectional view SEM images of the three-layer SiNW array (b) before transfer, (c) after first layer transfer, and (d) after second layer transfer. Insets in (c) and (d) show the photograph of the SiNW arrays on thermal release tapes.

transferred to the thermal release tape by peeling off the tape from the Si substrate. (iii) The third step is transfer of the SiNW array onto a target substrate. The SiNW array on the thermal release tape can be further transferred onto a counter-substrate via the same R2R method. Different from the R2R process in step i, the rollers of the laminating machine are heated to ∼120 °C in this process to release the SiNW array from the tape. Figure 4b shows the SEM image of the three-layer SiNW array before R2R transfer, while Figure 4c and Figure 4d depict the SEM images of the SiNW arrays after one-layer and two-layer transfer, respectively. Significantly, the cracked SiNW array can be layer-by-layer transferred to the tape via the facile R2R method. We note that the transfer is very thorough and does not make any damage to the underlying SiNW array. Photographs in the insets of Figure 4c and Figure 4d indicate that large-area uniform SiNW array can be obtained on the tape after transfer, verifying the high efficiency of the proposed R2R transfer method. On the other hand, from Figure S2a and Figure S2b, it is seen that the SiNW array can be further released from the tape to a flexible PET substrate under a roller temperature of ∼120 °C.

It is noteworthy that the wafer-scale transfer of the SiNW array can be achieved with the R2R transfer method. From Figure S3a and Figure S3b, it is seen that the cracked SiNW array on the 4 in. Si wafer is perfectly transferred to the thermal release tape via R2R transfer. SEM images taken from different locations of 1−4 on thermal release tape also demonstrate that the SiNW arrays are remarkably uniform, irrespective of the locations on the tape. The demonstration of wafer-scale transfer of the SiNW array to a flexible and low-cost substrate is essential to their future applications in electronic, sensor, and energy conversion devices.

Figure 5a shows the SEM image of the transferred SiNW array on thermal release tape, indicating that to a large extent the NWs can retain the vertical alignment on the tape. This is particularly important for their practical applications, since most of the distinct properties of the nanostructure arrays, such as light-trapping effect, are related to their highly ordered alignment. Figure 5b depicts the reflectance spectrum of the transferred SiNW array on tape, along with the spectra of planar Si wafer and an as-prepared SiNW array for comparison. Notably, the reflectance of the transferred SiNW array is much lower than that of the planar Si, while is comparable to that of the as-prepared SiNW array on Si wafer. This result clearly demonstrates that the transferred SiNW array on tape can still maintain the excellent anti-light-reflection property.

Recycle of the Si Substrate. The thickness of commercial Si wafer is usually in the range of 400−500 μm (Figure 6a). Even after three-layer SiNW array etching, as shown in Figure 6b, the remaining Si substrate still has a thickness of ∼380 μm. This means that most of the Si material will be dissipated if only the top two-layer SiNW arrays were transferred and utilized (the bottom SiNW array connects in series with the Si substrate and cannot be transferred by R2R method, as shown in Figure 6c). Therefore, in order to make the full use of the Si wafer, reutilization of the remaining Si substrate is critically important and much desired. There are two methods to achieve the reutilization of the Si wafer. In first method, newly three-layer SiNW array was fabricated via continued etching on the remaining Si substrate without introduction of any new Ag catalyst. This method no doubt allows the maximum reutilization of the Si substrate. However, as shown in Figure 6d, the structure uniformity of newly fabricated three-layer SiNW array is much worse than that of the SiNW array obtained from the original Si substrate. This result is likely attributed to the large consumption of the Ag catalyst during the first three-layer SiNW array etching; the left Ag catalyst is too little to support another round of three-layer SiNW array etching. Alternatively, in the second method, the remaining Si substrate was polished before second-round etching, and ∼40

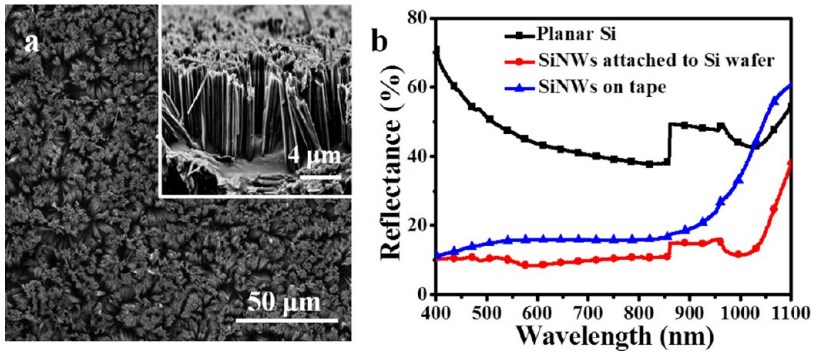

Figure 5. (a) Top-view SEM image of the transferred SiNW array on thermal release tape. Inset shows the cross-sectional view SEM of the SiNW array on tape. (b) Reflectance spectrum of the transferred SiNW array on tape. The reflectance spectra for planar Si and as-prepared SiNW array on Si wafer were also measured for comparison.

dx.doi.org/10.1021/am4043883 | ACS Appl. Mater. Interfaces 2014, 6, 977−984

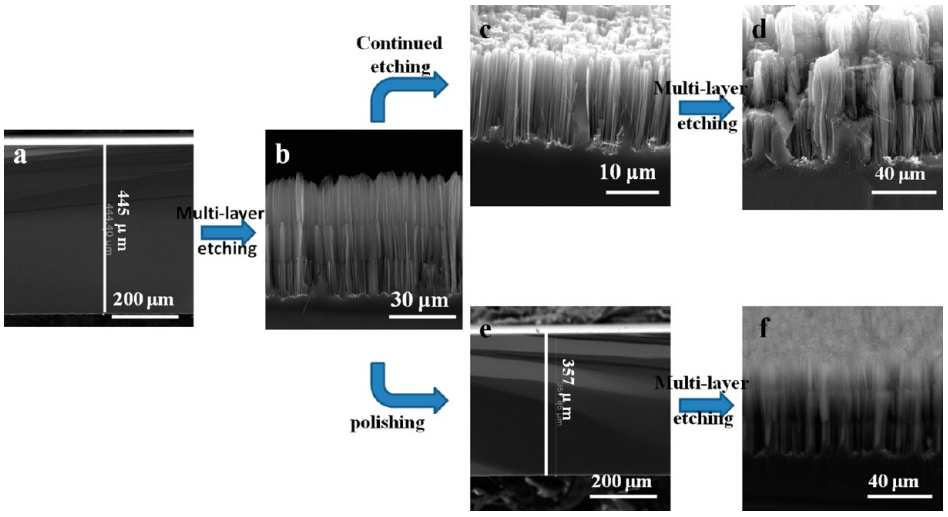

Figure 6. (a) Si wafer before etching. The thickness of the original Si wafer is 445 μm. (b) Three-layer SiNW array fabricated on Si wafer after etching. (c) Si substrate after the transfer of the top two-layer SiNW arrays. The bottom SiNW array was left on the Si substrate, since it connected in series with the substrate and cannot be transferred. (d) Newly three-layer SiNW array fabricated by continued etching of the remaining Si substrate in (c). It is noted that no new Ag catalyst was introduced in this process. The etching was sustained by the residual Ag catalyst in (c). (e) Polished Si substrate after SiNW array transfer with a thickness of ~357 μm. (f) Newly three-layer SiNW array fabricated on the polished Si substrate.

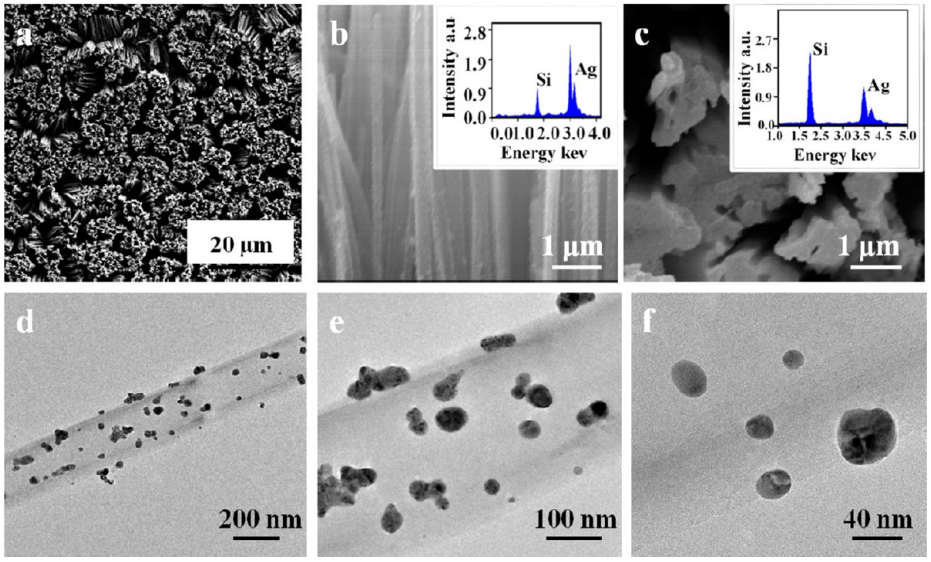

Figure 7. (a) Top-view SEM image of the freshly transferred SiNWs on thermal release tape. (b) Side-view and (c) top-view SEM images of the Ag NPs-modified SiNW array. Insets show the corresponding EDS spectra. (d–f) TEM images of the AgNPs-modified SiNW.

μm Si material was lost during the polishing process (Figure 6e). Afterward, newly three-layer SiNW array was fabricated on the polished Si substrate (Figure 6f). Notably, the SiNW array fabricated by this means has the same structure uniformity as that fabricated on the original Si substrate, in contrast to the SiNW array fabricated on unpolished Si substrate. This result implies that the polishing method is superior to the continued etching method, though some Si material will be lost in the polishing process.

SERS Applications of Transferred SiNW Arrays. SiNWs can serve as excellent candidates for sensors partly because they are environmentally friendly, biologically compatible, easy to prepare, and convenient to modify.[30] As we know, to apply SERS in routine studies for molecular sensing purpose, SERS substrates should be stable, reproducible, inexpensive, and easy to fabricate. Noble metals, such as Ag and Au, can be readily reduced and coated on the surface of H-terminated SiNWs; hence, Ag/Au NPs modified SiNWs can serve as excellent substrates for SERS applications. In previous reports, SiNWs coated with various metals, such as Ag, Cu, Pd, Co, Au, and Pt NPs,[12] have been employed and exhibited high sensitivity for molecule detection.[13,31] In comparison to the SiNW array on rigid substrate, the flexible SiNW array on tape has the advantages of low cost, small thickness, and light weight and therefore possesses great potential for SERS applications. To exploit it, we took the widely used R6G as the model molecule, and the SiNW array on tape was modified with AgNPs (denoted as Ag@SiNWs) to enhance the SERS signals.

Figure 7a shows the freshly transferred SiNWs on tape. After modification, the SiNWs retain the vertical aligned array structure, as shown in Figure 7b and Figure 7c. Strong Ag signals appear in the EDS spectra taken from the top and side

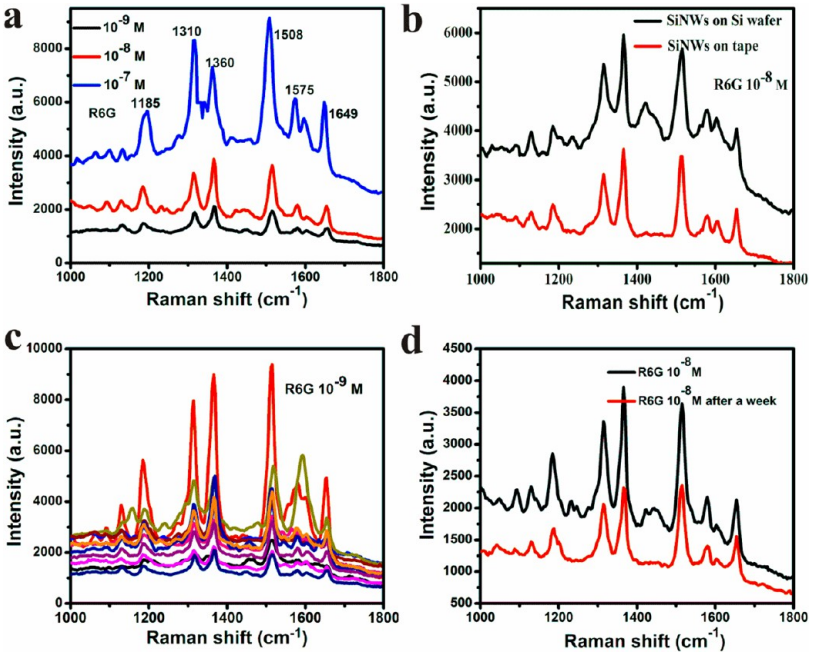

Figure 8. (a) Raman spectra collected from the flexible Ag@SiNWs with varied R6G concentrations of 10^{-7}, 10^{-8}, and 10^{-9} M. (b) Raman spectra collected from the Ag@SiNWs on Si substrate and the flexible Ag@SiNWs with R6G concentration of 10^{-8} M. (c) SERS spectra of 10^{-9} M R6G from 13 randomly selected positions on the optimized flexible Ag@SiNWs substrate under identical experimental conditions. (d) Raman spectra collected from the same substrate when it is freshly prepared and placed in the air for a week.

surfaces of the SiNW array, certifying the successful deposition of AgNPs on it. TEM analysis also discloses that the AgNPs have sizes in the range of 10−50 nm and are uniformly distributed on the SiNW surface (Figure 7d−f). This is very conductive to the SERS applications of the flexible Ag@SiNWs.

Figure 8 shows the SERS results collected by dropping 5 μL of methanol solution that contains various amounts of R6G molecules on the flexible AgNPs-modified SiNW array. From Figure 8a, pronounced scattering peaks at 1185, 1310, 1360, 1508, 1575, and 1649 cm^{-1}, which correspond to the symmetric in-plane C−C stretching vibrations of R6G, can be readily identified. It is evident that the flexible Ag@SiNWs substrate possesses excellent SERS activity. The highest intensity of Raman signal was collected when the target molecule concentration was 10^{-7} M, while the detection limit could be as low as 10^{-9} M. Figure 8b shows the Raman spectra collected from both the Ag@SiNWs attached to Si substrate and the Ag@SiNWs transferred to flexible tape. We note that they show nearly identical Raman spectra, indicating that the transfer process and the change of the support substrate have little influence on the SERS activity of the Ag@SiNWs, and the ∼10 μm thick SiNW array on the tape is sufficient to provide a high detection sensitivity. We also calculate the SERS enhancement factor (EF) to characterize the SERS effect, which is defined as[32,33]

$$\mathrm{EF} = (I_{\mathrm{surf}}N_{\mathrm{bulk}})/(I_{\mathrm{bulk}}N_{\mathrm{surf}})$$

where I_{surf} and I_{bulk} are the peak intensities for the SERS measurements with 10^{-9} M R6G on Ag@SiNWs substrate and for the normal Raman measurement with 10^{-3} M R6G solution dispersed on Si wafer, respectively. N_{surf} and N_{bulk} are the number of molecules on the SERS substrate and that on Si wafer illuminated by the laser light. Here, the Raman band at 1360 cm^{-1} is chosen. The highest I_{surf} intensity from 13 randomly selected positions on SERS substrate is 6200 (Figure 8c), while the I_{bulk} is 845 from Figure S4. Since both the N_{bulk} and N_{surf} are mainly determined by the concentration under the given volume and area, the ratio of N_{bulk} to N_{surf} can be estimated from the ratio of the concentrations. As a result, an optimum EF value of 7.34×10^6 can be deduced for the Ag@SiNWs substrate. We note that this value is comparable to previous reports on SiNWs based SERS substrates.[34,35]

To test whether the flexible Ag@SiNWs substrates is able to give reproducible SERS signals, we collected SERS spectra of 10^{-9} M R6G from 13 randomly selected positions on the optimized Ag@SiNWs substrate under identical experimental conditions, as shown in Figure 8c. Interestingly, the Raman spectra collected at different positions have similar intensity, revealing the excellent reproducibility of the SERS substrate. Figure 8d depicts the Raman spectra collected from the same substrate when it is freshly prepared and after placing in the air for 1 week, respectively. Notably, neither a shift in the major Raman peaks nor a significant change in Raman intensity occur for the SERS spectra after the 1-week storage, revealing that the flexible Ag@SiNWs substrate is stable in air. Besides R6G, both PATP and CV were used as the probe molecules, and the results are depicted in Figure S5. It is noteworthy that the flexible Ag@SiNWs are also capable of detecting PATP and CV molecules with relatively high sensitivity. The above results unambiguously demonstrate the great potential of the flexible Ag@SiNWs as high-sensitivity SERS substrates for molecule detection.

CONCLUSIONS

In summary, we developed a simple yet efficient air heating route to achieve multilayer etched SiNW array. Heating to the as-prepared SiNW array in air made part of the Ag-catalyst melt; the adhesion of AgNPs at side surfaces of SiNWs resulted in the formation of a horizontal crack at the subsequent etching step. By repetition of the etching−air heating−etching steps,

dx.doi.org/10.1021/am4043883 | ACS Appl. Mater. Interfaces 2014, 6, 977−984

multilayer SiNW array with layer number up to 5 was successfully fabricated. Moreover, the dissipation of the Si material in conventional method could be effectively avoided through recycling of the etched Si substrate after polishing. Significantly, we demonstrated the layer-by-layer transfer of the cracked SiNW array via the R2R technique. The use of the thermal release tape in the R2R transfer is critical, since it has appropriate stickiness at room temperature, while the stickiness can be greatly reduced by heating to a temperature above 120 °C, offering the possibility to further transfer the SiNW array to any type of receiving substrate. As a demonstration of the promising applications, the flexible SiNW array was modified with AgNPs and served as SERS substrate for R6G molecule detection. Preliminary study indicated a high sensitivity of the flexible Ag@SiNWs substrate with a detection limit as low as 10^{-9} M. It is believed that the realization of multilayer etching and R2R transfer of the SiNW arrays will greatly promote their applications in sensors.

■ ASSOCIATED CONTENT

Ⓢ Supporting Information

SEM images of the cracked SiNW arrays fabricated by the hot water soaking method, SEM images of the SiNW array released from the thermal release tape to flexible PET substrate, wafer-scale transfer of the cracked SiNW array via R2R method, Raman spectra collected from the non-SERS substrate of Si wafer with R6G concentration of 10^{-3} M, and Raman spectra collected from the flexible Ag@SiNWs substrates with PATP concentration of 10^{-5} M and CV concentration of 10^{-7} M. This material is available free of charge via the Internet at http://pubs.acs.org.

■ AUTHOR INFORMATION

Corresponding Authors

*Xiujuan Zhang: phone, +86-512-65880955; e-mail, xjzhang@suda.edu.cn.

*Jiansheng Jie: phone, +86-512-65881265; e-mail, jsjie@suda.edu.cn.

Author Contributions

The manuscript was written through contributions of all authors. All authors have given approval to the final version of the manuscript.

Notes

The authors declare no competing financial interest.

■ ACKNOWLEDGMENTS

This work was supported by National Basic Research Program of China (973 Program, Grants 2012CB932400 and 2013CB933500), Major Research Plan of the National Natural Science Foundation of China (Grants 91027021 and 91233110), and National Natural Science Foundation of China (Grants 51173124 and 51172151).

■ REFERENCES

(1) Huang, M. H.; Mao, S.; Feick, H. H.; Yan, Q. Y.; Wu, Y.; Kind, H.; Weber, E.; Russo, R.; Yang, P. D. *Science* **2001**, *2*, 1897−1899.
(2) Duan, X. F.; Huang, Y.; Agarwal, R.; Lieber, C. M. *Nature* **2003**, *4*, 241−245.
(3) Bian, L.; Zhang, X. W.; Luan, C.Y.; Zapien, J. A.; Zhang, X. Z.; Wu, Y. M.; Jie, J. S. *J. Mater. Chem. A* **2013**, *1*, 6313−6319.
(4) Hochbaum, A. I.; Yang, P. D. *Chem. Rev.* **2010**, *110*, 527−546.
(5) Law, M.; Goldberger, J.; Yang, P. D. *Annu. Rev. Mater. Res.* **2004**, *34*, 83−122.
(6) Garnett, E. C.; Yang, P. D. *Nano Lett.* **2010**, *10*, 1082−1087.
(7) Kayes, B. M.; Atwater, H. A.; Lewis, N. S. *J. Appl. Phys.* **2005**, *97*, 114302.
(8) Kempa, T. J.; Tian, B. Z.; Kim, D. R.; Hu, J. S.; Zheng, X. L.; Lieber, C. M. *Nano Lett.* **2008**, *8*, 3456−3460.
(9) Zhang, X. Z.; Xie, C.; Jie, J. S.; Zhang, W. J. *J. Mater. Chem. A* **2013**, *1*, 6593−6601.
(10) Shen, X. J.; Sun, B. Q.; Liu, D.; Lee, S. T. *J. Am. Chem. Soc.* **2011**, *133*, 19408−19415.
(11) Zhang, F. T.; Song, T.; Sun, B. Q. *Nanotechnolgy* **2012**, *23*, 194006.
(12) Shao, M. W.; Ma, D. D.; Lee, S. T. *Eur. J. Inorg. Chem.* **2010**, *27*, 4264−4278.
(13) Fang, C.; Agarwal, A.; Widjaja, E.; Garland, M. V.; Wong, S. M.; Linn, L.; Khalid, N. M.; Salim, S. M.; Balasubramanian, N. *Chem. Mater.* **2009**, *21*, 3542−3548.
(14) Gudiksen, M. S.; Lauhon, L. J.; Wang, J. F.; Smith, D. C.; Lieber, C. M. *Nature* **2002**, *415*, 617−620.
(15) Yang, C.; Zhong, Z.; Lieber, C. M. *Science* **2005**, *310*, 1304−1307.
(16) Wu, Y.; Cui, Y.; Huynh, L.; Barrelet, C. J.; Bell, D. C.; Lieber, C. M. *Nano Lett.* **2004**, *4*, 433−436.
(17) Hochbaum, A.I.; Fan, R.; He, R. R.; Yang, P. D. *Nano Lett.* **2005**, *5*, 457−460.
(18) Peng, K. Q.; Yan, Y. J.; Gao, S. P.; Zhu, J. *Adv. Mater.* **2002**, *14*, 1164−1167.
(19) Smith, P. A.; Nordquist, C. D.; Jackson, T. N.; Mayer, T. S.; Martin, B. R.; Mbindyo, J.; Mallouk, T. E. *Appl. Phys. Lett.* **2000**, *77*, 1399−1401.
(20) Weisse, J. M.; Lee, C. H.; Kim, D. R.; Zheng, X. L. *Nano Lett.* **2012**, *12*, 3339−3343.
(21) Fan, Z. Y.; Ho, J. C.; Jacobson, Z. A.; Yerushalmi, R.; Alley, R. L.; Razavi, H.; Javey, A. *Nano Lett.* **2008**, *8*, 20−25.
(22) Weisse, J. M.; Kim, D. R.; Lee, C. H.; Zheng, X. L. *Nano Lett.* **2011**, *11*, 1300−1305.
(23) Sun, Y.; Rogers, J. A. *Adv. Mater.* **2007**, *19*, 1897−1916.
(24) Plass, K. E.; Filler, M. A.; Spurgeon, J. M.; Kayes, B. M.; Maldonado, S.; Atwater, B. S. H. A.; Lewis, N. S. *Adv. Mater.* **2009**, *21*, 325−328.
(25) Spurgeon, J. M.; Boettcher, S. W.; Kelzenberg, M. D.; Brunschwig, B. S.; Atwater, H. A.; Lewis, N. S. *Adv. Mater.* **2010**, *22*, 3277−3281.
(26) Ray, K.; Badugu, R. J.; Lakowicz, R. *J. Am. Chem. Soc.* **2006**, *128*, 8998−8999.
(27) Zhang, B. H.; Wang, H. S.; Lu, L.; Ai, K. L.; Zhang, G.; Cheng, X. L. *Adv. Funct. Mater.* **2008**, *18*, 2348−2355.
(28) Zhang, M. L.; Peng, K. Q.; Fan, X.; Jie, J. S.; Zhang, R. Q.; Lee, S. T.; Wong, N. B. *J. Phys. Chem. C* **2008**, *112*, 4444−4450.
(29) Moon, K. S.; Dong, H.; Maric, R.; Pothukuchi, S.; Hant, A.; Li, Y.; Wong, C. P. *J. Electron. Mater.* **2005**, *34*, 168−175.
(30) Peng, F.; Su, Y. Y.; Wei, X. P.; Lu, Y. M.; Zhou, Y. F.; Zhong, Y. L.; Lee, S. T.; He, Y. *Angew. Chem., Int. Ed.* **2013**, *52*, 1457−1461.
(31) Zhang, M. L.; Fan, X.; Zhou, H. W.; Shao, M. W.; Zapien, J. A.; Wong, N. B.; Lee, S. T. *J. Phys. Chem. C* **2010**, *114*, 1969−1975.
(32) Ru, L. E. C.; Blackie, E.; Meyer, M.; Etchegoin, P. G. *J. Phys. Chem. C* **2007**, *111*, 13794−13803.
(33) Wang, X. T.; She, G. W.; Mu, L. X.; Lee, S. T. *Appl. Phys. Lett.* **2010**, *96*, 053104.
(34) Lu, R.; Sha, J.; Xia, W.; Fang, Y. J.; Gu, L.; Wang, Y. W. *CrystEngComm* **2013**, *15*, 6207−6212.
(35) Jiang, X. X.; Jiang, Z. Y.; Xu, T. T.; Su, S.; Zhong, Y. L.; Peng, F.; Su, Y. Y.; He, Y. *Anal. Chem.* **2013**, *85*, 2809−2816.